European Journal of Medicinal Chemistry 66 (2013) 364–371

Contents lists available at SciVerse ScienceDirect

European Journal of Medicinal Chemistry

journal homepage: http://www.elsevier.com/locate/ejmech

Original article

Synthesis and bioevaluation of a series of α-pyrone derivatives as potent activators of Nrf2/ARE pathway (part I)

Mei-yang Xi [b,d,1], Zhong-ying Sun [c,1], Hao-peng Sun [a,b,d,**], Jian-min Jia [b,d], Zheng-yu Jiang [b,d], Lei Tao [c], Ming Ye [c], Xi Yang [c], Ya-jing Wang [c], Xin Xue [b,d], Jing-jie Huang [b,d], Yuan Gao [c], Xiao-ke Guo [b,d], Sheng-lie Zhang [b,d], Ying-rui Yang [b,d], Qing-long Guo [c], Rong Hu [c,***], Qi-dong You [a,b,*]

[a] State Key Laboratory of Natural Medicines, China Pharmaceutical University, Nanjing 210009, China
[b] Jiang Su Key Laboratory of Drug Design and Optimization, China Pharmaceutical University, Nanjing 210009, China
[c] Department of Physiology, School of Pharmacy, China Pharmaceutical University, Nanjing, China
[d] Department of Medicinal Chemistry, China Pharmaceutical University, Nanjing 210009, China

ARTICLE INFO

Article history:
Received 3 April 2013
Received in revised form
22 May 2013
Accepted 5 June 2013
Available online 14 June 2013

Keywords:
Nrf2
Keap1
ARE
α-Pyrone derivative
Chemopreventive agents

ABSTRACT

When exposed to electrophiles, human colorectal cancer cells (HCT116) counteract oxidative stress through activating NF-E2-related factor 2 (Nrf2)/antioxidant response element (ARE) pathway. To identify new activators, luciferase reporter gene assay was used to screen in-house database of our laboratory, leading to a novel α-pyrone compound **1** as a hit. **2** with 2-fluoro phenyl group exhibited the strongest ARE inductive activity in the first round structure–activity relationship (SAR) study. Biological studies showed the compound induced nuclear translocation of Nrf2 preceded by phosphorylation of ERK1/2. The data encouraged us to use **2** as lead and 20 derivatives were synthesized to discuss a more detailed SAR, leading to a more potent compound **9**, which can be the starting compound for further modification.

1. Introduction

Despite the enormous progress in the early detection and treatment of cancer, the high mortality for most cancers has not decreased in the past three decades [1]. As a new therapeutic strategy, chemoprevention is proved to be attractive in the modulation of the carcinogenesis process in recent years [2–4]. Many data from animal models have demonstrated that chemoprevention hinders the development of cancer [5–9]. Additionally, it is also confirmed to be effective in reducing the incidence of cancer in the well-defined high-risk groups [2,10]. Thus, chemoprevention deserves further attention.

Molecular biological investigations have shown that NF-E2-related factor 2 (Nrf2)/Kelch-like ECH-associated protein 1 (Keap1)/ARE pathway plays a crucial role in cancer chemoprevention [11]. It serves as the core in the complicated and efficient cyto-protective machinery in response to a variety of oxidative or electrophilic challenges in eukaryotic cells [12,13] and demonstrate that Nrf2 is a potential molecular target for cancer chemoprevention [14–16].

Nrf2 is a 66-kDa transcription factor which contains a Cap 'n' Collar (CNC) structure. It belongs to basic-leucine zipper (bZIP) transcription factor family (Fig. 1A). Nrf2 is considered to be one of the most important regulators during the chemoprevention process. In quiescent condition, Nrf2 is sequestered in cytoplasm by Keap1, a 69-kDa cytosolic protein usually existing as a dimer (Fig. 1B) [17], promoting its ubiquitination and degradation (Fig. 1C) [18]. However, under stress such as irritant, some mercapto groups of cysteine (cys) in Keap1 were oxidized or alkylated, changing the binding conformation of Keap1-Nrf2 complex. The degradation

* Corresponding author. China Pharmaceutical University, Tongjiaxiang 24, Nanjing 210009, China. Tel./fax: +86 25 83271351.
** Corresponding author. China Pharmaceutical University, Tongjiaxiang 24, Nanjing 210009, China. Tel./fax: +86 25 83271216.
*** Corresponding author. China Pharmaceutical University, Tongjiaxiang 24, Nanjing 210009, China. Tel./fax: +86 25 83271126.
E-mail addresses: sunhaopeng@163.com (H.-p. Sun), michelhu@hotmail.com (R. Hu), youqidong@gmail.com (Q.-d. You).
[1] These two authors contributed equally to this work.

0223-5234/$ – see front matter © 2013 Elsevier Masson SAS. All rights reserved.
http://dx.doi.org/10.1016/j.ejmech.2013.06.007

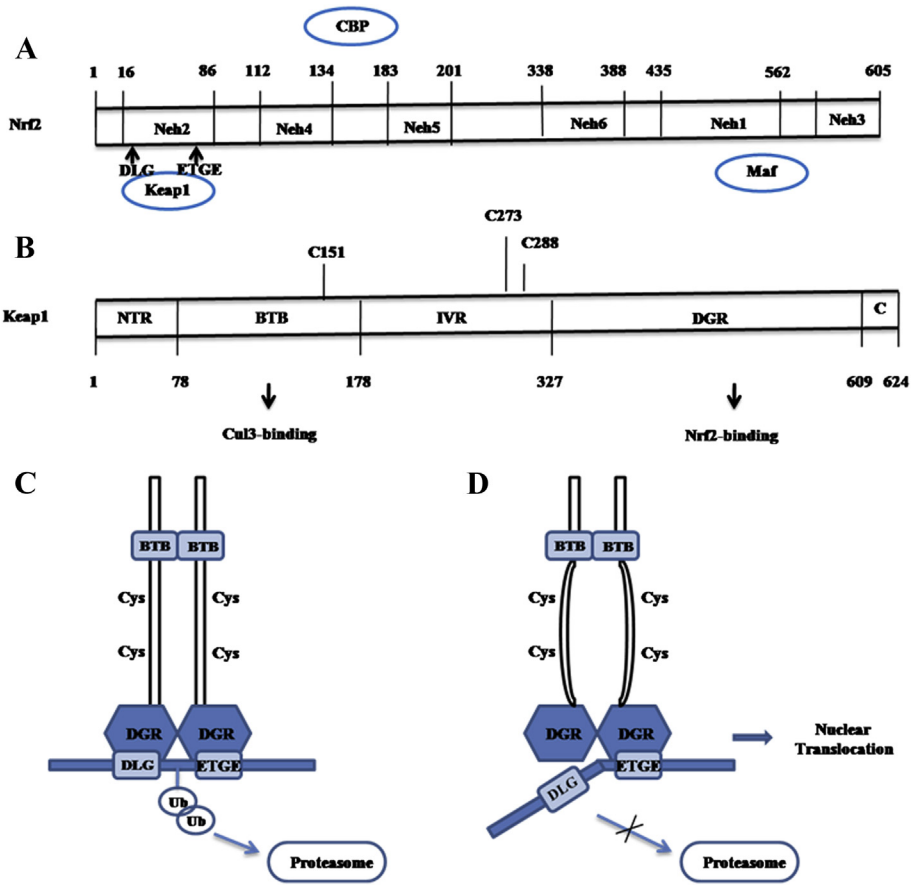

Fig. 1. Structure of Nrf2, Keap1; the "hinge and latch" two-site binding model is proposed and mercapto group of cys in Keap1 is modified, in favor of DLG dissociation. (A) The Neh2 contains DLG and ETGE for binding Keap1. Neh4 and 5 bind a coactivator CBP. Neh1 binds Maf and DNA. (B) The BTB mediates homodimerization. In BTB and IVR, Cys151, 273 and 288 are important for Nrf2 dissociating from Keap1. DGR consists of 6 Kelch motifs for Nrf2 binding. (C) Without cellular stress, Nrf2 is bound by Keap1. Homodimer DGR domain of Keap1 interacts with DLG and ETGE motifs of Nrf2, enabling ubiquitination and proteasomal degradation. (D) Under some oxidative stress, the low-affinity DLG "latch" is disconnected. Nevertheless, the high-affinity ETGE "hinge" is kept. As a result, non-degradable Nrf2 and saturated Keap1 cause that any new Nrf2 is capable of translocating to the nuclei.

process of Nrf2 is then prohibited, leading to the accumulation of newly synthesized Nrf2. It then translocates to the nuclei and dimerizes with Maf. The dimerized protein binds to ARE promotors, recruits CREB-binding protein (CBP), induces transcription and upregulates the expression of phase-II enzymes such as heme oxygenase-1 (HO-1) and NAD(P)H:quinone oxidoreductase 1 (NQO-1) (Fig. 1D) [19].

Due to the significant role of Nrf2 in the chemoprevention process, compounds inducing ARE activation through Nrf2/Keap1 pathway are attractive and considered to be chemopreventive agents [11,20,21]. These compounds are blocking agents for the tumor initiation phase and suppressing agents for the tumor promotion and progression phase [22,23]. Till now, there are several classes of ARE inducers reported. Most of them are separated from dietary food, such as curcumin, EGCG, resveratrol, genistein and sulforaphane (Fig. 2) [24]. A common structure of α, β-unsaturated ketone plays a key role in the chemopreventive activity of these compounds. With this information in hand, in the present study, a structural similarity screening of our in-house natural product database was performed in order to discover novel chemopreventive agents. A compound with α-pyrone scaffold, exhibiting strong ARE inducer activity, was confirmed as lead compound through several bioevaluations. Two rounds of molecular optimization were carried out to study the structure–activity relationship (SAR), leading to more potent derivatives.

2. Results

2.1. Chemistry

In order to identify the action pathway of the hit **1**, we designed and synthesized 25 derivatives **2**–**26** (Table 1). The synthetic route

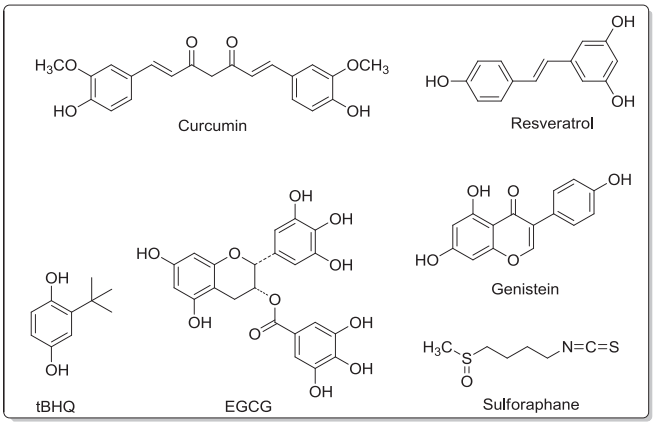

Fig. 2. The structure of chemopreventive agents.

Table 1
The activity of compounds **1**–**26**.

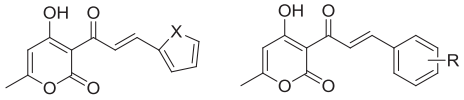

Compd. ID	R/X	Inductivity (concentration/μM)		IC_{50}/μM	PKa	Log P	Log D7.4
		50	20		Predicted		
1	H	6.84 ± 0.89	4.21 ± 0.29	>100	5.18	2.39	0.19
2	2-F	3.04 ± 0.34	7.08 ± 0.17	>100	5.11	2.45	0.18
3	S	5.96 ± 0.08	4.53 ± 0.68	>100	5.11	2.20	−0.06
4	O	5.48 ± 0.03	3.80 ± 0.32	>100	5.11/16.55/−0.48	2.01	−0.25
5	NH	3.58 ± 0.37	1.66 ± 0.04	>100	5.11	0.92	−1.34
6	2-NO_2	0.65 ± 0.22	2.74 ± 0.52	>100	5.10	1.94	−0.34
7	3-F	3.46 ± 0.58	7.04 ± 0.29	81.18 ± 6.11	5.12	2.51	0.25
8	4-F	5.79 ± 1.08	6.33 ± 0.47	>100	5.13	2.40	0.15
9	3,4-F	3.68 ± 0.47	9.65 ± 0.82	74.87 ± 8.04	5.09	2.43	0.15
10	2,4-F	6.98 ± 0.55	6.93 ± 1.11	80.33 ± 6.05	5.10	2.49	0.22
11	3-Cl	4.51 ± 1.22	6.46 ± 1.06	66.35 ± 4.05	5.12	2.99	0.73
12	4-Cl	6.28 ± 1.37	6.97 ± 1.07	87.41 ± 6.55	5.12	2.91	0.66
13	2,4-Cl	3.27 ± 0.30	5.49 ± 0.96	88.72 ± 7.09	5.09	3.31	1.02
14	3,4-Cl	1.20 ± 0.37	8.00 ± 0.44	>100	5.10	3.39	1.12
15	4-OCH_3	7.37 ± 0.95	6.48 ± 0.24	>100	5.13	2.33	0.09
16	4-OCH_2CH_3	5.50 ± 0.06	4.66 ± 1.13	>100	5.14	2.87	0.63
17	2,4-OCH_3	6.81 ± 0.31	8.21 ± 0.86	>100	5.12	2.22	−0.04
18	3,4,5-OCH_3	5.25 ± 0.08	8.58 ± 0.43	>100	5.11	1.98	−0.29
19	2-Naphthyl	2.17 ± 0.23	1.37 ± 0.72	>100	5.13	3.62	1.37
20	4-Phenyl	3.60 ± 0.54	5.67 ± 0.05	>100	5.12	4.15	1.89
21	4-$N(CH_3)_2$	8.09 ± 0.23	4.55 ± 0.50	>100	5.16/5.11	2.90	0.67
22	4-NO_2	2.48 ± 0.34	4.77 ± 0.14	65.02 ± 3.90	5.09	2.17	−0.11
23	4-CN	2.07 ± 0.24	3.68 ± 0.76	66.03 ± 6.92	5.11	1.96	−0.31
24	2-Cl	0.95 ± 0.15	5.08 ± 0.25	>100	5.11	2.77	0.50
25	2-OCH_3	2.08 ± 0.16	5.86 ± 0.67	>100	5.12	2.39	0.13
26	2-CF_3	2.55 ± 0.13	4.27 ± 0.42	>100	5.11	3.36	1.09
^{t}BHQ		5.08 ± 0.06 (80 μM)		>100	12.99/10.80	2.33	2.33
DMSO		1 ± 0.05					

HepG2-ARE-C8 cells were treated with the compounds or ^{t}BHQ or DMSO for 12 h followed by luciferase assays. The ARE inducer activity was shown as a ratio to the DMSO control. Predicted values of PKa, Log *P*, Log *D*7.4 were used ACDLABS PRO software.

is summarized in Scheme 1. Briefly, α-pyrone **27** (4-hydroxy-6-methyl-2-pyrone) was acetylated with acetic acid in the presence of DCC, DMAP to obtain **28** in 86.4% yield. Addition of intermediate **28** with substituted aromatic aldehyde produced the target compounds in about 62% yield.

2.2. Screening results

2.2.1. ARE inductivity

For the screening, we explored ARE inductivity of the compounds using luciferase reporter gene assays at 20 and 50 μM on a 96-well plate in HepG2-ARE-C8 cells. Compound **1** with a α-pyrone scaffold was identified as a hit. It showed >4-fold induction of ARE compared to the control group. The cytotoxic activity of the hit was determined through the 3-(4,5-dimethylthiazol-2-yl)-2,5-diphenyltetrazol-ium-bromide (MTT) method in HCT116 cells (Table 1).

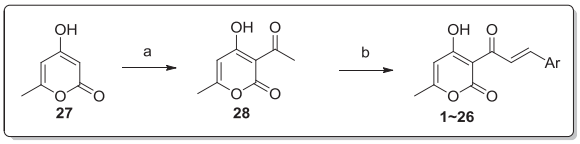

Reagents and conditions: (a) DCC, DMAP, CH_3COOH, 100 ℃, 2 h; (b) aromatic aldehyde, piperidine, CH_3Cl_3, 24 h.

Scheme 1. The synthetic route of compound **1**–**26**.

2.2.2. First round SAR and mechanism of α-pyrone derivatives

For the preliminary SAR study (Scheme 2), five compounds (**2**–**6**) with different groups were synthesized. They were tested at 20, 50 μM in their ability to elevate ARE levels in HepG2-ARE-C8 cells (12 h treatments, Table 1). When the phenyl in compound **1** was substituted by the furan (**4**) or pyrrole group (**5**), the activity was decreased. The thienyl substituted compound (**3**) exhibited equal potency as **1**. The activity of these compounds was concentration dependent. Interestingly, while substituted with 2-fluoro phenyl ring (**2**), the compound remarkably enhanced ARE activation at 20 μM compared to **1**. However, the ARE inductivity decreased at 50 μM. According to above results, **2** was used to do biological mechanism study.

We determined the ARE activation by **2** at the concentration of 2.5, 5, 10, 20 and 30 μM, and no apparent cytotoxicity was observed. **2** increased ARE inductivity in a concentration dependent manner (Fig. 3).

We tested the expression of Nrf2 and phase II enzymes such as HO-1 and NQO-1 after treatment with **2**. The compound maximized the expression of HO-1 and NQO-1 at 8 h and 24 h, respectively, while induction of Nrf2 reached a stable state after 2 h (Fig. 4). As Nrf2 could activate the expression of downstream phase II enzymes after nuclear translocation, we isolated nuclear and cytoplasmic fractions after treatment with **2** and determined Nrf2 levels. Nrf2 nuclear localization was first seen at 1 h, while decreasing at 24 h (Fig. 5).

The activities of several kinases, including MAPK, PI3K, PKC, CK2, and PERK, are implicated in the regulation of Nrf2 activity.

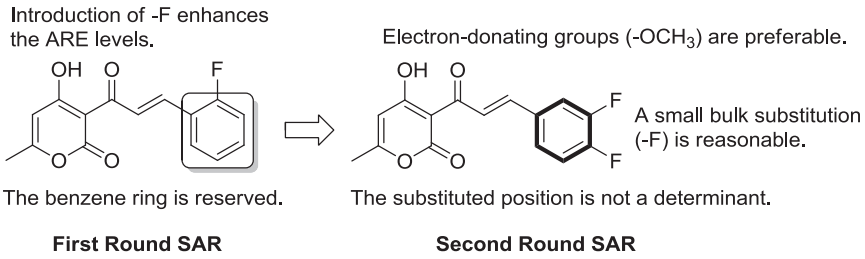

[a] Two rounds SAR study is shown above via totally synthesizing 25 compounds **2**-**26**.

Scheme 2. The SAR of α-pyrone derivatives.[a]

It has been also shown that the kinases involved in phosphorylation and activation of Nrf2 appear to be cell type dependent [19]. To investigate whether some signal transduction is required for **2** to activate the ARE levels, 4 kinase inhibitors were chosen to separately cotreat with **2** to during the determination of ARE inductivity (Fig. 6). While cotreated with a MEK1/2 inhibitor **PD98059**, the ARE inductive activity of **2** was blocked obviously [25]. Therefore, subsequent experiments were implemented with **PD98059**.

Our study indicated that the compound **2** can affect the activity of ERK1/2 signal transduction pathway by regulating phosphorylation process of ERK1/2. Exposure to the compound **2** resulted in a rapid and sustained activation (phosphorylation) of ERK1/2. Activation of ERK1/2 was obvious as early as 30 min and maximized at 1 h. On the other hand, the expression of ERK1/2 protein was not altered. The compound mediated activation of ERK1/2 was additionally confirmed by determining phosphorylation of the ERK1/2 downstream substrates (Fig. 7A).

Additionally, cotreatment with a MEK1/2 inhibitor, **PD98059** (20 μM), blocked activation of ERK1/2 but not ERK1/2 itself, significantly attenuated Nrf2, HO-1 and NQO-1 protein upregulation with addition of **2** (Fig. 7B), suggesting that Nrf2 activation partly attribute to transient activation of ERK1/2 by the compound **2**.

Based on immunofluorescence experiment, we obtained that the compound **2** activated the transcription factor Nrf2 signaling pathway 1 h later. Subsequently, Nrf2 was continuously enhanced for 2 h. The data indicated an increased translocation of Nrf2 into the nuclei after the treatment of **2**. After blocking ERK1/2 with **PD98059** in 1 and 2 h respectively, we found that Nrf2 nuclear translocation was decreased at both indicated times (Fig. 7C). These phenomena also demonstrated that the compound **2** which exhibited Nrf2 inductivity was proceded by activating ERK1/2 signal pathway.

2.3. Second round SAR of α-pyrone derivatives that induce ARE activation

After the above mechanism research, we designed and synthesized another 20 derivatives **7**–**26** to study the detailed SAR (Scheme 2) and identify a more potent ARE inducer. The IC_{50} value and ARE inductivity of **7**–**26** are shown in Table 1. In general, the optimal compound was **9** with an approximately 10-fold increase at 20 μM in ARE levels as compared to control followed by **18**, **17**, **14** and **2**.

For substituted groups on benzene ring, we firstly considered the steric effect. With regard to naphthyl substitution (**19**), the inductivity decreased sharply. This may due to the binding pocket was not large enough for naphthyl binding. The data also suggested that the binding pocket was a long and narrow area, because the biphenyl compound (**20**) showed acceptable activity. The preferable binding mode may need phenyl substituted with some spatially small groups, such as halogen, methoxyl or hydroxyl group. As a result, we synthesized a series of compounds with these substituted groups. According to the biological results, the compounds with halogens (−F or −Cl) and −OCH_3 substitution had preferable inductivity compared to other compounds. The substituted position at the benzene ring was not key element for the higher activity. Specially, it was worth paying attention to compounds with −F substitution (**2**, **7**, **8**, **9** and **10**) because of their strong ARE enhancement. The data also indicated that −F substitution was a privileged molecular optimization strategy to enhance the Nrf2 inductive activity for these compounds. Furthermore, the activity with di-halogens substitution (**9**, **14**) was prior to those single substituted compounds.

For −OCH_3 substitution, the activity was as follows: tri-substitution (**18**) > di-substitution (**17**) > single substitution (**15**, **25**). The higher activity of **15** *vs* **16** showed a potential steric hindrance at 4-position. It also indicated that the steric effects of the substituted groups at the benzene ring need to be carefully considered.

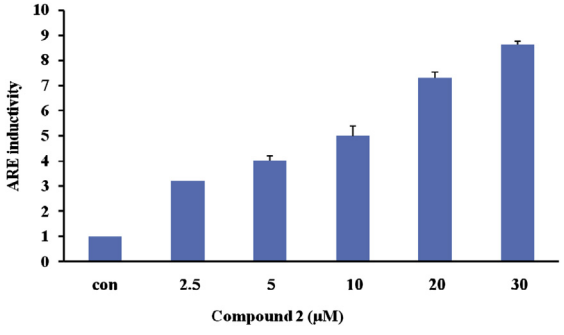

Fig. 3. The ARE inductivity of the compound **2**. HepG2-ARE-C8 cells were treated with the compounds or DMSO for 12 h. The activity was shown as a ratio to the DMSO control (con). Data are expressed as mean ± SD ($n = 3$).

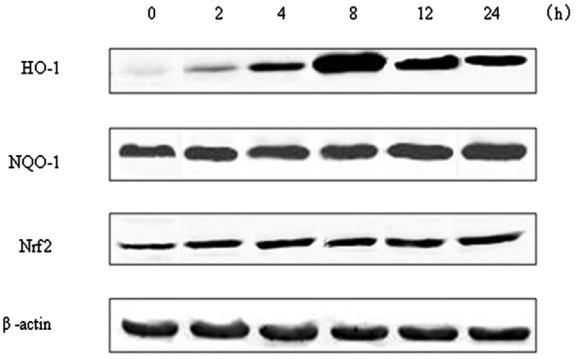

Fig. 4. Time-dependent expression of HO-1, NQO-1 and Nrf2 affected by the compound **2**. After treatment with **2** (20 μM), cell lysates were prepared from HCT116 cells and subjected to Western blot analysis.

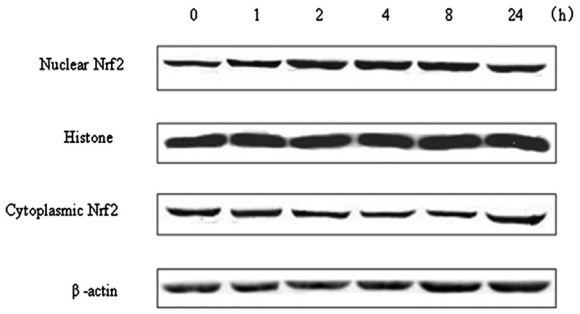

Fig. 5. Effects of **2** on nuclear translocation of Nrf2. After treatment with **2** (20 μM), nuclear and cytoplasmic cell extracts were prepared from HCT116 cells and subjected to western blot analysis for Nrf2, histone and β-actin. nuclear translocation initiated within 1 h and reached a plateau after 2 h.

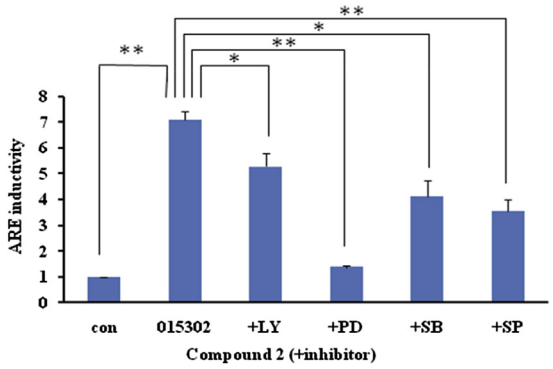

Fig. 6. The activity of **2** (20 μM) is inhibited when the ERK1/2 pathway is blocked. Cotreatment with inhibitors of either PI3K (**LY294002**, 10 μM), MEK1 (**PD098059**, 20 μM), P38 (**SB203580**, 5 μM) or JNK (**SP600125**, 5 μM) for 12 h, HepG2-ARE-C8 cells were followed by luciferase assay. The activity was shown as a ratio to the DMSO control (con). Data are expressed as mean ± SD ($n = 3$). Differences are statistically significant at $^{*}p < 0.05$, $^{**}p < 0.01$.

Secondly, we considered the electrostatic effect of the substituted groups. With $-NO_2$ (**6**), $-OCH_3$ (**25**) or $-CF_3$ (**26**) substitution at 2-position and with $-OCH_3$ (**15**), $-NO_2$ (**22**) or $-CN$ (**23**) substitution at 4-position, the activity (at 20 μM) decreased dramatically, indicating the electrostatic state of the substituted groups affected critically to the Nrf2 inductive activity. Additionally, electron-withdrawing groups also showed toxicity at a high concentration, which also explained the decrease of the activity. On the contrary, electron-donating groups showed promising activity except for $-N(CH_3)_2$ (**21**) substitution. This may be due to the steric effect. Besides, electron-donating groups such as $-OCH_3$ (**15**) and $-N(CH_3)_2$ (**21**) substitution showed much lower cytotoxicity, as the activity was concentration dependent obviously.

In a word, **9** exhibited the highest ARE inductivity. **015314**, **015317** and **015318** are also excellent ARE inducers. To identify physicochemical property, lipo-hydro partition coefficient was predicted. High Log *P* value of **14** and low Log $D_{7.4}$ value of **17**, **18** was disadvantages to druggability. To improve it, some hydrogen bond acceptors or donors can be added in the following years. Thus, on the basis of these data, we can select compound **9** for further analysis.

3. Discussion

Expression of the Nrf2/ARE-induced enzymes by some chemical molecules, which detoxify potential electrophiles and oxidants, indicates a promising strategy for cancer chemoprevention. In this point, many potent chemopreventive agents with various types of structures have been identified [26]. In the present study, we searched our in-house compound database for novel Nrf2/ARE activators by using cytotoxity assay and luciferase measurement. A potent compound **1** with α-pyrone chemical skeleton was identified and five derivatives were synthesized for the first round SAR study. These compounds were tested for their Nrf2/ARE induction activity using HepG2-ARE-C8 cells. The potent compound **2**, with −F substituted at *ortho*-position, was much more potent than the

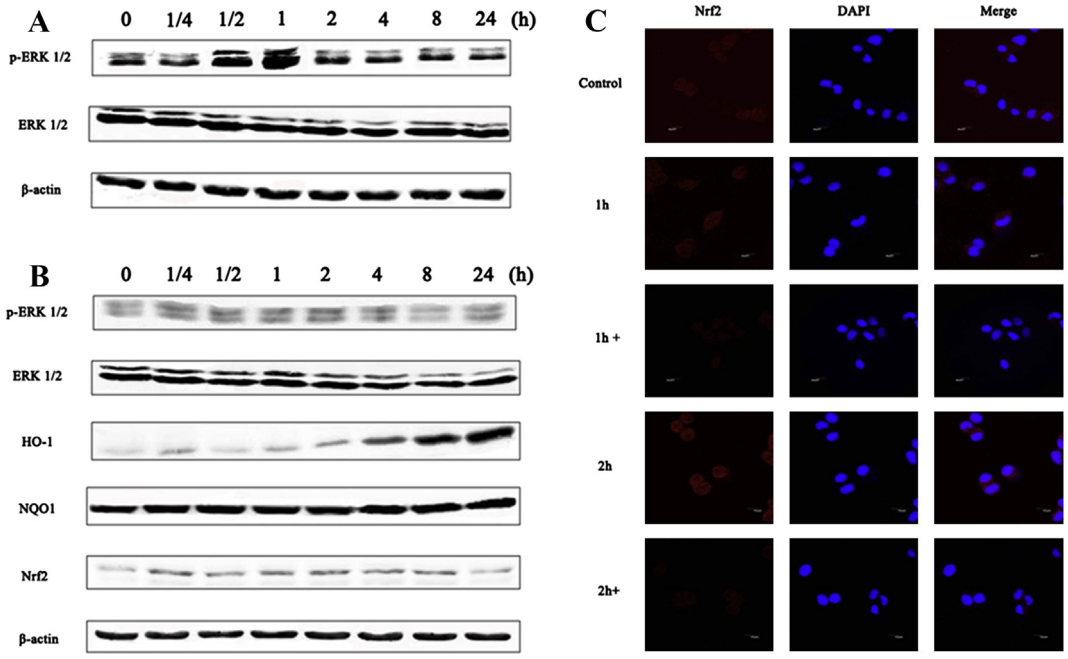

Fig. 7. Effects of **2** (20 μM) on ERK1/2 signal transduction. (A) At indicated times after treatment with **2** (20 μM), cell lysates were prepared from HCT116 cells and subjected to western blot analysis for phosphorylated and total ERK1/2. (B) Cotreatment with the MEK1/2 inhibitor, **PD98059** (20 μM), HCT116 cells were subjected to western blot analysis for phosphorylated ERK1/2, total ERK1/2, Nrf2, HO-1 and NQO-1. (C) Immunofluorescence staining of Nrf2 in indicated treatment in HCT116 cells. Nrf2 and nuclei was labeled with Cy3 and DAPI, respectively. Red: Nrf2; Blue: nuclei. 1 h, 2 h: treatment with **2** (20 μM); 1 h+, 2 h+: cotreatment with **PD98059** (20 μM). Bars inserted indicate magnification (10 μm). (For interpretation of the references to color in this figure legend, the reader is referred to the web version of this article.)

positive control ^{t}BHQ. Meanwhile, the toxicity of the compounds was also evaluated by MTT method. The IC_{50} values of these compounds were much higher than the concentration that led to Nrf2/ARE induction, proving the safety of our compounds.

In the following mechanism study, we found that **2** up-regulates the expression of NQO-1, HO-1 and promotes Nrf2 translocation into the nuclei. NQO-1 plays an important role in protecting cells against ROS [27]. HO-1 possesses anti-inflammatory, anti-oxidative and anti-apoptotic activity [28,29]. The induction of the HO-1 and NQO-1 gene is regulated mostly via the Nrf2/ARE pathway as it includes a variety of ARE sequences in its promoter. Additionally, the expression of Nrf2 can be induced through some signaling pathways, such as mitogen-activated protein kinases (MAPKs) and PI3K/Akt [25,30–33]. Based on these facts, we tested four upstream kinases by cotreated **2** with the corresponding kinase inhibitor respectively. We found the expression of Nrf2 and downstream enzymes induced by **2** was mainly mediated by ERK1/2. Moreover, covalent modification of the sulfhydryl of Keap1 is proposed as another molecular mechanism in Nrf2/ARE activation. For example, sulforaphane and CAPE are speculated to interact with the sulfhydryl and activate the Nrf2/ARE pathway [34,35]. As an electrophilic agent possessing α, β-unsaturated carbonyl groups, it is required to testify whether **2** can interact with the sulfhydryl group in later experiments. Twenty derivatives of **2** were further synthesized and evaluated for a second round SAR study. Among them, **9** exhibits much better potency in the induction of ARE activity than **2**. Further analysis can be developed around the promising compound **9**.

4. Conclusion

We screened in-house database of our laboratory by luciferase reporter gene assay aimed at identifying a novel small molecule which is a potential activator in Nrf2/ARE pathway. **1** was chosen as a hit. Structural modification and preliminary SAR investigation was in progress, as well as molecular mechanism. The results presented herein support the hypothesis that **2** is a potent chemopreventive agent. Furthermore, up-regulation in the level of phosphorylated ERK1/2 is shown to be associated with transcription factor Nrf2 activation accompanied by HO-1, NQO-1 induction. By using the first round of SAR information in cooperate with biological assay to estimate the inductivity of second round of synthesized compounds, we discovered the promising compound **9**, planning to optimize the SAR, study underlying mechanism for chemoprevention and explore the target as a chemopreventive agent. Accordingly, the compound **9** may protect cells against oxidative stress. We conclude that ARE activators described here may be valuable in preventing cells from irritants.

5. Experimental procedures

5.1. Chemistry

All reagents were from commercial sources. With tetramethylsilane (TMS) as internal standard, the ^{1}H NMR was recorded on Bruker AV-300 apparatus by using deuterated solvents. EI-MS was collected on Shimadzu GCMS-2010 instruments. Every target compound was purified via silica gel (60 Å, 70–230 mesh) column chromatography. Melting points were measured by XT-4 melting point apparatus.

5.1.1. 3-Acetyl-4-hydroxy-6-methyl-2-pyrone (*28*)

To a solution of **27** (5.0 g, 40.0 mmol) in toluene (60.0 mL), DMAP (1.0 g, 8.0 mmol), acetic acid (2.4 g, 40.0 mmol), DCC (8.2 g, 40.0 mmol) were added. The reaction mixture was stirred at 100 °C for 2 h, then the organic solution was evaporated. The crude product was purified by using column chromatography (PE:EtOAc = 5:1) to afford 5.8 g **28** as light yellow solid. Yield: 86.4%.

5.1.2. The general synthetic procedure of target compound *1–26*

In a two-necked flask, the *ortho*-substituted benzaldehyde (3.0 mmol), piperidine (2 d) and the intermediate 2 (3.0 mmol) were dissolved in chloroform (4.0 mL), and the mixture was stirred for reflux. After 12 h, the mixture was monitored by TLC using 20% petroleum ether/ethyl acetate as the developing solvent system. The reaction was stopped and then the mixture was evaporated and crystallized with ethanol.

*5.1.2.1. (E)-1-(3-Acetyl-4-hydroxy-6-methyl-2-pyrone)-3-(3,4-difluoro-phenyl)-2-en-1-one (**9**).* It was obtained as a yellow solid in 43.5% yield. ^{1}H NMR (300 MHz, $CDCl_3$): δ 2.30 (s, 3H), 5.98 (s, 1H), 7.12–7.51 (m, 3H), 7.82 (d, J = 15.8 Hz, 1H), 8.22 (d, J = 15.8 Hz, 1H); ^{13}C NMR (CDCl3): δ 191.97, 182.46, 168.54, 160.65, 153.13, 151.87, 142.92, 125.34, 123.67, 117.49, 117.25, 116.88, 116.66, 101.72, 20.15.; m/z (EI-MS): 292 $[M]^+$; HRMS (ESI): calcd. for $C_{15}H_{11}F_2O_4$ $[M + H]^+$ 293.062, found 293.0634. m.p. 160–161 °C.

*5.1.2.2. (E)-1-(3-Acetyl-4-hydroxy-6-methyl-2-pyrone)-3-(2,4-difluoro-phenyl)-2-en-1-one (**10**).* It was obtained as a yellow solid in 51.2% yield. ^{1}H NMR (300 MHz, $CDCl_3$): δ 2.22 (s, 3H), 5.91 (s, 1H), 6.77–6.90 (m, 2H), 7.66–7.71 (m, 1H), 7.99 (d, J = 15.9 Hz, 1H), 8.23 (d, J = 15.9 Hz, 1H); m/z (EI-MS): 292 $[M]^+$; HRMS (ESI): calcd. for $C_{15}H_{11}F_2O_4$ $[M + H]^+$ 293.062, found 293.0632. m.p. 173–174 °C.

*5.1.2.3. (E)-1-(3-Acetyl-4-hydroxy-6-methyl-2-pyrone)-3-(2- naphthalene)-2-en-1-one (**19**).* It was obtained as a yellow solid in 47.3% yield. ^{1}H NMR (300 MHz, $CDCl_3$): δ 2.05 (s, 3H), 5.56 (s, 1H), 7.54–8.01 (m, 7H), 8.07 (d, J = 15.7 Hz, 1H), 8.36 (d, J = 15.7 Hz, 1H); m/z (EI-MS): 306 $[M]^+$; HRMS (ESI): calcd. for $C_{19}H_{15}O_4$ $[M + H]^+$ 307.0965, found 307.0974. m.p. 176–178 °C. The data of known compounds were presented in the Supporting information.

5.2. Biology

5.2.1. Cell culture conditions

HepG2 cells stably transfected with ARE luciferase reporter (HepG2-ARE-C8) were kindly provided by Professor Dr. A. N. Tony Kong (Rutgers University, Piscataway, NJ). Cells were maintained in modified RPMI-1640 medium (GiBco, USA) with 10% fetal bovine serum (FBS) (GiBco, USA) in a humidified atmosphere of 5% CO_2 and 95% air at 37 °C. HCT116 cells (Cell Bank of Shanghai Institute of Biochemistry and Cell Biology, Shanghai Institutes for Biological Sciences, Chinese Academy of Sciences) were cultured in McCoy's 5A (Sigma–Aldrich, USA) supplemented with 10% (v/v) FBS.

5.2.2. MTT analysis

Cell viabilities were determined by using MTT assay. MTT was purchased from Sigma (St. Louis, MO). It was dissolved in phosphate buffered saline (PBS) to a concentration of 5 mg/mL as the stock solution and stored at −20 °C. After cells were exposed with different concentrations of test compounds, 20 μL of MTT solution was added into 96-well plates for 4 h. Then the solution was removed and 100 μL of DMSO was added into each well, The OD values were determined at 570 nm by Elx800 Absorbance Microplate Reader (BioTek, Vermont, USA).

$$IC_{50} = [1 - (OD_{test} - OD_{blank})/(OD_{control} - OD_{blank})]*100\%.$$

5.2.3. ARE-luciferase activity assay

HepG2-ARE-C8 cells were plated in 96-well plates at a density of 4×10^4 cells/well and incubated overnight. The cells were exposed with different concentrations of test compounds, with ^{t}BHQ serving as a positive control DMSO as a negative control and the luciferase cell culture lysis reagent as a blank. In some experiments, cells were cotreated with inhibitors of either MEK1 (**PD098059**, 20 μM), PI3K (**LY294002**, 10 μM), P38 (**SB203580**, 5 μM) (Beyotime, China) or JNK (**SP600125**, 5 μM) (Sigma–Aldrich, USA). After 12 h of treatment, the medium was removed and 100 μL of cold PBS was added into each well. Then the cells were harvested in the luciferase cell culture lysis reagent. After centrifugation, 20 μL of the supernatant was used for determining the luciferase activity according to the protocol provided by the manufacturer (Promega, Madison, WI). The luciferase activity was measured by a luminoskan ascent (Thermo scientific, USA). The data were obtained in triplicates and expressed as fold induction over control.

$$\text{Inductivity} = (\text{RLU}_{\text{test}} - \text{RLU}_{\text{blank}})/(\text{RLU}_{\text{control}} - \text{RLU}_{\text{blank}}).\ \text{RLU} = \text{relative light unit}.$$

5.2.4. Western blot

Anti-HO-1 (sc-136960) and -NQO1 (sc-271116) antibodies were from Santa Cruz Biotechnology (Santa Cruz, CA, USA). Anti-β-actin (AP0060) and -Nrf2 (BS1258) were purchased from Bioworlde (Bioworlde, USA). Antibodies against p-erk1/2 (#4370) and erk1/2 (#4695) were obtained from Cell Signaling Technology (Beverly, MA, USA). Cells were washed once with ice-cold PBS and driven down with 2 mL of EDTA. Cells were centrifuged at 2500 rpm and resuspended in 45 μL of Lysis buffer, which was composed of 50 mM Tris–HCl, 150 mM NaCl, NP-40, 1 mM EDTA, PMSF, NaF, Leu and DTT for 1 h. Then cells were centrifuged again at 12,000 rpm for 20 min at 4 °C. The supernatant was retained, and the protein concentration was determined by the BCA assay with Varioskan flash (Thermo, Waltham, MA) at 562 nm. Samples were stored at −80 °C until use. Nuclear and cytosol were isolated using the nuclear-cytosol extraction kit (KeyGEN, NJ, China). Then the separate extracts were stored at −80 °C until use. The extracts were separated by SDS–PAGE and then transferred onto PVDF membranes (Perkin Elmer, Northwalk, CT, USA). After blocking with 1% BSA for 2 h, membranes were incubated at 37 °C for 1 h and then at 4 °C overnight with a primary antibody. After that, they were reacted with a DyLight 800 labeled secondary antibody at 37 °C for 1 h. The membranes were screened through the odyssey Infrared Imaging System (LI-COR, Lincoln, Nebraska, USA).

5.2.5. Immunofluorescence

Cells were cotreated with the compound **2** (20 μM) and inhibitors of MEK1 (**PD098059**, 20 μM), then incubated at 4 °C overnight with Nrf2 primary antibodies (abcam, UK). After washing with PBS, cells were incubated at 37 °C for 1 h with cy3-labeled secondary sheep anti-rabbit IgG antibody (BOSTER, Wh, China). Cells were then stained with fluorochrome dye DAPI (Santa Cruz Biotechnology, Santa Cruz, CA) to visualize the nuclei and observed under a laser scanning confocal microscope (Olympus Fluoview FV1000, Japan) with a peak excitation wave length of 570 nm and 340 nm.

Acknowledgments

This work was supported by the project 81230078 (Key Program), 81202463 (Youth Foundation) and 91129732 of National Natural Science Foundation of China, Program of State Key Laboratory of Natural Medicines, China Pharmaceutical University (No. JKGQ201103), 2012AA020301 of 863 program, 2010ZX09401-401 and 2009ZX09501-003 of the National Major Science and Technology Project of China (Innovation and Development of New Drugs). The authors declare no other conflicts of interest.

Appendix A. Supplementary data

Supplementary data related to this article can be found at http://dx.doi.org/10.1016/j.ejmech.2013.06.007.

References

[1] W.K. Hong, M.B. Sporn, Recent advances in chemoprevention of cancer, Science 278 (1997) 1073–1077.
[2] G.J. Kelloff, R. Lieberman, V.E. Steele, C.W. Boone, R.A. Lubet, L. Kopelovich, W.A. Malone, J.A. crowell, H.R. Higley, C.C. Sigma, Agents, biomarkers, and cohorts for chemopreventive agent development in prostate cancer, Urology 57 (2001) 46–51.
[3] T. Yamadori, Y. Ishii, S. Homma, Y. Morishima, K. Kurishima, K. Itoh, M. Yamamoto, Y. Minami, M. Noguchi, N. Hizama, Molecular mechanisms for the regulation of Nrf2-mediated cell proliferation in non-small-cell lung cancers, Oncogene 31 (2012) 4768–4777.
[4] S. Magesh, Y. Chen, L. Hu, Small molecule modulators of Keap1–Nrf2–ARE pathway as potential preventive and therapeutic agents, Med. Res. Rev. 32 (2012) 687–726.
[5] D.E. Corpet, F. Pierre, Point: from animal models to prevention of colon cancer. Systematic review of chemoprevention in min mice and choice of the model system, Cancer Epidemiol. Biomarkers Prev. 12 (2003) 391–400.
[6] B.S. Reddy, Studies with the azoxymethane-rat preclinical model for assessing colon tumor development and chemoprevention, Environ. Mol. Mutagen. 44 (2004) 26–35.
[7] C. Neufert, C. Becker, M.F. Neurath, An inducible mouse model of colon carcinogenesis for the analysis of sporadic and inflammation-driven tumor progression, Nat. Protoc. 2 (2007) 1998–2004.
[8] C. Stolfi, A. Rizzo, E. Fraze, A. Rotondi, M.C. Fantini, M. Sarra, R. Caruso, I. Monteleone, P. Sileri, L. Franceschilli, F. Caprioli, S. Ferrero, T.T. MacDonald, F. Pallone, G. Monteleone, Involvement of interleukin-21 in the regulation of colitis-associated colon cancer, J. Exp. Med. 208 (2011) 2279–2290.
[9] C.W. Barrett, B. Fingleton, A. Williams, W. Ning, M.A. Fischer, M.K. Washington, R. Chaturvedi, K.T. Wilson, S.W. Hiebert, S.W. Hiebert, C.S. Williams, MTGR1 is required for tumorigenesis in the murine AOM/DSS colitis-associated carcinoma model, Cancer Res. 71 (2011) 1302–1312.
[10] T. Kakizoe, Chemoprevention of cancer-focusing on clinical trials, Jpn. J. Clin. Oncol. 33 (2003) 421–442.
[11] C.R. Zhao, Z.H. Gao, X.J. Qu, Nrf2–ARE signaling pathway and natural products for cancer chemoprevention, Cancer Epidemiol. 34 (2010) 523–533.
[12] T. Ishii, K. Itoh, H. Sato, S. Bannai, Oxidative stress-inducible proteins in macrophages, Free Radic. Res. 31 (1999) 351–355.
[13] M.K. Kwak, P.A. Eqner, P.M. Dolan, M. Ramos-Gomez, J.D. Groopman, K. Itoh, M. Yamamoto, T.W. Kensler, Role of phase 2 enzyme induction in chemoprotection by dithiolethiones, Mutat. Res. 305 (2001) 480–481.
[14] W.S. Jeong, M. Jun, A.N. Kong, Nrf2: a potential molecular target for cancer chemoprevention by natural compounds, Antioxid. Redox Sign. 8 (2006) 99–106.
[15] H.K. Na, Y.J. Surh, Transcriptional regulation via cysteine thiol modification: a novel molecular strategy for chemoprevention and cytoprotection, Mol. Carcinog. 45 (2006) 368–380.
[16] J.S. Lee, Y.J. Surh, Nrf2 as a novel molecular target for chemoprevention, Cancer Lett. 224 (2005) 171–184.
[17] J.H. Wu, W. Miao, L.G. Hu, G. Batist, Identification and characterization of novel Nrf2 inducers designed to target the intervening region of Keap1, Chem. Biol. Drug Des. 75 (2010) 475–480.
[18] E. Balogun, M. Hoque, P. Gong, E. Killeen, C.J. Green, R. Foresti, J. Alam, R. Motterlini, Curcumin activates the haem oxygenase-1 gene via regulation of Nrf2 and the antioxidant-responsive element, Biochem. J. 371 (2003) 887–895.
[19] W. Hur, Z. Sun, T. Jiang, D.E. Mason, E.C. Peters, D.D. Zhang, H. Luesch, P.G. Schultz, N.S. Gray, A small-molecule inducer of the antioxidant response element, Chem. Biol. 17 (2010) 537–547.
[20] J.D. Hayes, M. McMahon, NRF2 and KEAP1 mutations:permanent activation of an adaptive response in cancer, Trends Biochem. Sci. 34 (2009) 176–188.
[21] I.M. Copple, C.E. Goldring, N.R. Kitteringham, B.K. Park, The Nrf2-Keap1 defence pathway: role in protection against drug-induced toxicity, Toxicology 246 (2008) 24–33.
[22] I. Berenblum, V. Armuth, Two independent aspects of tumor promotion, Biochim. Biophys. Acta 651 (1981) 51–63.
[23] C. Heidelberger, A.E. Freeman, R.J. Pienta, A. Sivak, J.S. Bertram, B.C. Casto, V.C. Dunkel, M.W. Francis, T. Kakunaga, J.B. Little, L.M. Schechtman, Cell transformation by chemical agents-a review and analysis of the literature.

A report of the U.S. Environmental Protection Agency Gene-Tox Program, Mutat. Res. 114 (1983) 283–385.
[24] R. Hu, C.L. Saw, R. Yu, A.N. Kong, Regulation of NF-E2-related factor 2 signaling for cancer chemoprevention antioxidant coupled with antiinflammatory, Antioxid. Redox Signal. 13 (2010) 1679–1698.
[25] T.O. Khor, S. Yu, A.N. Kong, Dietary cancer chemopreventive agents – targeting inflammation and Nrf2 signaling pathway, Planta. Med. 74 (2008) 1540–1547.
[26] R. Kachadourian, B.J. Day, S. Pugazhenti, C.C. Franklin, E. Genoux-Bastide, G. Mahaffey, C. Gauthier, A. Di Pietro, A. Boumendjel, A synthetic chalcone as a potent inducer of glutathione biosynthesis, J. Med. Chem. 55 (2012) 1382–1388.
[27] M.S. Yates, M. Tauchi, F. Katsuoka, K.C. Flanders, K.T. Liby, T. Honda, G.W. Gribble, D.A. Johnson, J.A. Johnson, N.C. Burton, T.R. Guilarte, M. Yamamoto, M.B. Sporn, T.W. Kensler, Pharmacodynamic characterization of chemopreventive triterpenoids as exceptionally potent inducers of Nrf2-regulated genes, Mole. Cancer Ther. 6 (2007) 154–162.
[28] A.K. Jaiswal, Regulation of genes encoding NAD(P)H: quinone oxidoreductases, Free Radic. Bio. Med. 29 (2000) 254–262.
[29] D. Willis, A.R. Moore, R. Frederick, D.A. Willoughby, Heme oxygenase: a novel target for the modulation of the inflammatory response, Nat. Med. 2 (1996) 87–93.
[30] A. Prawan, J.K. Kundu, Y.J. Surh, Molecular basis of heme oxygenase-1 induction: implications for chemoprevention and chemoprotection, Antioxid. Redox Sign 7 (2005) 1688–1703.
[31] Y. Zhang, L. Guan, X. Wang, T. Wen, J. Xing, J. Zhao, Protection of chlorophyllin against oxidative damage by inducing HO-1 and NQO1 expression mediated by PI3K/Akt and Nrf2, Free Radic. Res. 42 (2008) 362–371.
[32] M.H. Li, Y.N. Cha, Y.J. Surh, Peroxynitrite induces HO-1 expression via PI3K/Akt-dependent activation of NF-E2-related factor 2 in PC12 cells, Free Radic. Biol. Med. 41 (2006) 1079–1091.
[33] A. Tanaka, N. Hamada, Y. Fujita, T. Itoh, Y. Nozawa, M. Iinuma, M. Ito, A novel kavalactone derivative protects against H_2O_2-induced PC12 cell death via Nrf2/ARE activation, Bioorg. Med. Chem. 18 (2010) 3133–3139.
[34] J.H. Lim, K.M. Kim, S.W. Kim, O. Hwang, H.J. Choi, Bromocriptine activates NQO1 via Nrf2-PI3K/Akt signaling: novel cytoprotective mechanism against oxidative damage, Pharmacol. Res. 57 (2008) 325–331.
[35] A.T. Dinkova-Kostova, W.D. Holtzclaw, R.N. Cole, K. Itoh, N. Wakabayashi, Y. Katoh, M. Yamamoto, P. Talalay, Direct evidence that sulfhydryl groups of Keap1 are the sensors regulating induction of phase 2 enzymes that protect against carcinogens and oxidants, Proc. Natl. Acad. Sci. U. S. A. 99 (2002) 11908–11913.